SLL 80-226/P

NOVEMBER 1975
SAI-75-005-AA

INVESTIGATIONS IN SUPPORT OF HIGH ENERGY LASER TECHNOLOGY

FINAL REPORT

1 JULY 1974 TO 30 JUNE 1975

for

DEFENSE ADVANCED RESEARCH PROJECTS AGENCY/STO
ARLINGTON, VA 22209

CONTRACT DAAHO1-73-C-0786

Science Applications, Inc.
15 Research Dr., P.O. Box 328, Ann Arbor, MI 48107

NOTICES

Sponsorship. The work reported herein was conducted by Science Applications, Inc., Ann Arbor office, for the Defense Advanced Research Projects Agency of the Department of Defense and was monitored by the U. S. Army Missile Command under Contract Number DAAH01-73-C-0786, ARPA Order Number 1180. ARPA Program manager is Dr. Peter O. Clark. Project Manager is Dr. F. Haak.

Distribution. Initial distribution is indicated at the end of this document.

Accession Number: 3953

Publication Date: Nov 01, 1975

Title: Investigations in Support of High Energy Laser Technology

Personal Author: Smith, F.G.; Chang, T.S.; Meredith, R.E.; WIlson, C.W.

Corporate Author Or Publisher: Science Applications Inc., PO Box 328, Ann Arbor, MI 48107 Report Number: SAI-75-005-AA

Report Prepared for: U.S. Army Missile Command, Redstone Arsenal, AL 35809 Report Number Assigned by Contract Monitor: SLL 80-226

Comments on Document: Archive, RRI, DEW.

Descriptors, Keywords: Investigation Support High Energy Laser Technology Hydrogen Chloride Kinetics Sodium Argon Cross Relaxation Inhomogeneous Broadening Dissociation Alkali Noble Gas Performance Deactivation Vibration

Pages: 00050

Cataloged Date: Nov 30, 1990

Contract Number: DAAH01-73-C-0786

Document Type: HC

Number of Copies In Library: 000001

Record ID: 25344

Source of Document: DEW

Unclassified

SECURITY CLASSIFICATION OF THIS PAGE (When Data Entered)

REPORT DOCUMENTATION PAGE		READ INSTRUCTIONS BEFORE COMPLETING FORM
1. REPORT NUMBER SAI-75-005-AA	2. GOVT ACCESSION NO.	3. RECIPIENT'S CATALOG NUMBER
4. TITLE (and Subtitle) Investigations in Support of High Energy Laser Technology		5. TYPE OF REPORT & PERIOD COVERED Final Report 1 July 1974 to 30 June 1975 6. PERFORMING ORG. REPORT NUMBER
7. AUTHOR(s) F. G. Smith, T. S. Chang, R. E. Meredith and C. W. Wilson		8. CONTRACT OR GRANT NUMBER(s) DAAH01-73-C-0786
9. PERFORMING ORGANIZATION NAME AND ADDRESS Science Applications, Inc. P. O. Box 328 Ann Arbor, MI 48107		10. PROGRAM ELEMENT, PROJECT, TASK AREA & WORK UNIT NUMBERS ARPA Order 1180
11. CONTROLLING OFFICE NAME AND ADDRESS Defense Advanced Research Projects Agency/STO 1400 Wilson Boulevard Arlington, VA 22209		12. REPORT DATE November 1975 13. NUMBER OF PAGES 50
14. MONITORING AGENCY NAME & ADDRESS(if different from Controlling Office) U. S. Army Missile Command Redstone Arsenal, AL 35809		15. SECURITY CLASS. (of this report) Unclassified 15a. DECLASSIFICATION/DOWNGRADING SCHEDULE

16. DISTRIBUTION STATEMENT (of this Report)

17. DISTRIBUTION STATEMENT (of the abstract entered in Block 20, if different from Report)

18. SUPPLEMENTARY NOTES

Principal Investigator, R. E. Meredith.

19. KEY WORDS (Continue on reverse side if necessary and identify by block number)

HCL Laser Kinetics
NaAr
Cross Relaxation
Inhomogeneous Broadening
Dissociation Laser

20. ABSTRACT (Continue on reverse side if necessary and identify by block number)

Three investigations of fundamental laser kinetic processes have been performed: H atom deactivation of HCl in the H_2-HCl transfer laser, the effects of inhomogeneous broadening and cross relaxation on laser performance, and the chemistry of NaAr formation, for application to rare gas-alkali laser development.

DD FORM 1 JAN 73 1473 EDITION OF 1 NOV 65 IS OBSOLETE

Unclassified

SECURITY CLASSIFICATION OF THIS PAGE (When Data Entered)

20. ABSTRACT (Continued)

The temperature dependence of the deactivation of HCl v = 1 level has been mapped from 300° K to 1000° K and the vibrational state dependence has been computed at 500° K. Results suggest that the deactivation energy has the value -316 cal/mole. Relative rates of the deactivation of the higher states show that multiquantum collisional cooling is important, contrary to the usual assumption.

The homogeneous broadening parameter f_{osc} has been evaluated for ten potential HEL candidates including the rare gas mono-halide, KrF, which operates at about 250 nm. It is concluded that infrared lasers operating at typical pressure and temperature conditions should not suffer from inhomogeneous broadening effects, but that short wavelength lasers could very well be affected.

Extensive ab initio and semi-empirical calculations of NaAr potential functions have been performed. Results indicate that the bound $A\,^2\pi$ state results mainly from an ion-induced dipole interaction with possible contribution from Van der Waals forces. It has been found that the variation of the transition moment with internuclear separation has a significant effect on the gain of the medium.

NOVEMBER 1975

SAI-75-005-AA

INVESTIGATIONS IN SUPPORT OF HIGH ENERGY LASER TECHNOLOGY

FINAL REPORT

1 July 1974 to 30 June 1975

for

DEFENSE ADVANCED RESEARCH PROJECTS AGENCY/STO
ARLINGTON, VA 22209

CONTRACT DAAH01-73-C-0786

SCIENCE APPLICATIONS, INC.
15 Research Drive, P.O. Box 328, Ann Arbor, MI 48107

TABLE OF CONTENTS

FIGURES

TABLES

INVESTIGATIONS IN SUPPORT OF HIGH ENERGY LASER TECHNOLOGY

1.0 INTRODUCTION

During the past several years, a series of analytical investigations into the physics and chemistry of various laser media has been performed. Early in the program, line-width measurements of HF broadening by various gases were analyzed, and the results were used to do an extensive set of calculations of both HF and DF line widths at chemical laser cavity conditions for gain-profile modeling. This study of the broadening of laser molecular line profiles led to an investigation of inhomogeneous broadening and cross relaxation of the laser gain profile. Recent results of this study are in this report. Also included here are calculations of the vibration deactivation of HCl by H atoms. This study is significant for modeling the promising non-reacting mixing laser which would operate on the HCl vibration transitions in the infrared.

Investigations of potential visible laser molecules have been a continuing part of the present program. The visible laser studies have been fundamental in nature and have mainly addressed the alkali-noble gas laser media. Results of these calculations are included in the present volume along with some applications of the inhomogeneous broadening formulation to visible laser systems.

2.0 H ATOM DEACTIVATION OF HCl VIBRATION

Lasing from the vibrationally excited states of HCl has been achieved by a variety of excitation mechanisms. These mechanisms produce vibrationally hot and rotationally cold HCl; thereby achieving lasing in the P branch of the vibrational transitions.

The maintenance of this disparity between the vibrational and rotational temperatures is paramount to device performance. Cooling processes inherent to the laser medium or to the excitation mechanism limit achievable device performance. One formidable coolant present in HCl laser media is the H atom. This specie is always produced by the rapid dissociation of HCl arising from its elevated vibrational temperature. Several excitation mechanisms produce additional H atoms, e.g., the chain reactions operative in the chemical laser devices require the presence of H atoms. In the nonreacting mixing laser [1], H atoms are produced in the vibrational heating of the H_2 pumping gas. Hydrogen atoms are generally present in HCl laser media. Models of proposed high-power HCl lasers show the effect of H atoms to be a dramatic reduction in performance; therefore, their cooling effects must be considered in the engineering of high performance HCl laser devices.

Available data is insufficient for the modelling of high energy devices. The room temperature rate of the process

$$H + HCl\ (v=1) \longrightarrow H + HCl\ (v=0) \qquad (1)$$

has been measured [2]. Theoretical attempts [3] to extrapolate this datum to other conditions have been unreliable, and only qualitative empirical

extrapolations have been employed in device modelling. The present study provides a reliable theoretical determination of the temperature dependence of the measured process. In addition, the detailed rates of deactivation of the higher states v=2 and 3 are related to the v=1 to v=0 process.

2. 1. Potential Energy Surfaces

As pointed out above, there is a dearth of data on the collisions of H atoms with HCl. (Extrapolation from a single data point is hardly justified.) Fortunately, considerable data is available on the related reactive process

$$H_2 + Cl \longrightarrow HCl + H. \qquad (2)$$

These data have been analyzed to extract the potential operative during reactive encounters [4], a related aspect of the potential controlling collisions of H atoms with HCl molecules. From these data, the potential controlling collisions of the atom with the H end of the molecule is known. Attack on the opposite end of the molecule samples regions of the potential which play no role in the reaction; hence, those segments of the potential are unknown.

In the absence of adequate empirical data on this region of the surface, calculation of the potential is a viable alternative for the determination of the potential. The Diatomics-in-Molecules [5] potential for this region was found to exhibit an 11 kcal/mole barrier to the H atom exchange process in the linear symmetric geometry at an H-Cl separation of 1.46 Å. Similar calculations [6] show a 16 kcal/mole barrier in the F analogue of this system. In contrast, accurate ab initio calculations [7] indicate the barrier there is in excess of 40 kcal/mole. Thus, the DIM barrier height is suspect, and the actual

barrier may be considerably higher than the 11 kcal/mole DIM prediction. Scaling the ab initio barrier in H F H using the DIM formalism suggests a 28 kcal/mole barrier is present in the H-Cl-H system. The LEPS potential function used in the scattering calculation exhibits an 8 kcal/mole well in this region [8] and is clearly erroneous there. Collisions striking the Cl end of the molecule will be predicted to undergo direct H atom exchange rather than simple elastic collision. (Mass factors make inelastic processes improbable.) For the analysis these collisions have simply been neglected to simulate the effect of the missing barrier; the inelastic processes of interest occur in the known region of the potential. Therefore, the empirical potential is adequate.

2. 2. Kinetics Calculations

Classical scattering calculations on this potential surface have been used to estimate the kinetics of H atom deactivation of HCl vibration. These calculations have been performed using an extensively modified version of Polanyi's REACT2 code [9]. These revisions included recoding of the numerical integration sections to improve the efficiency of trajectory tracking, changes in the Monte-Carlo selection of representative collisions, and insertion of an analysis routine specific to the present problem.

Analysis of the calculations yields rate data pertinent to modelling of HCl laser cavity chemistry. The thermal rate of reactive consumption of HCl by H

$$H + HCl \longrightarrow H_2 + Cl \qquad (3)$$

is found to be slow (1.0×10^{-12} cm^3/sec at 1000^oK); however, this rate rises exponentially with HCl vibrational state (see Figure 1).

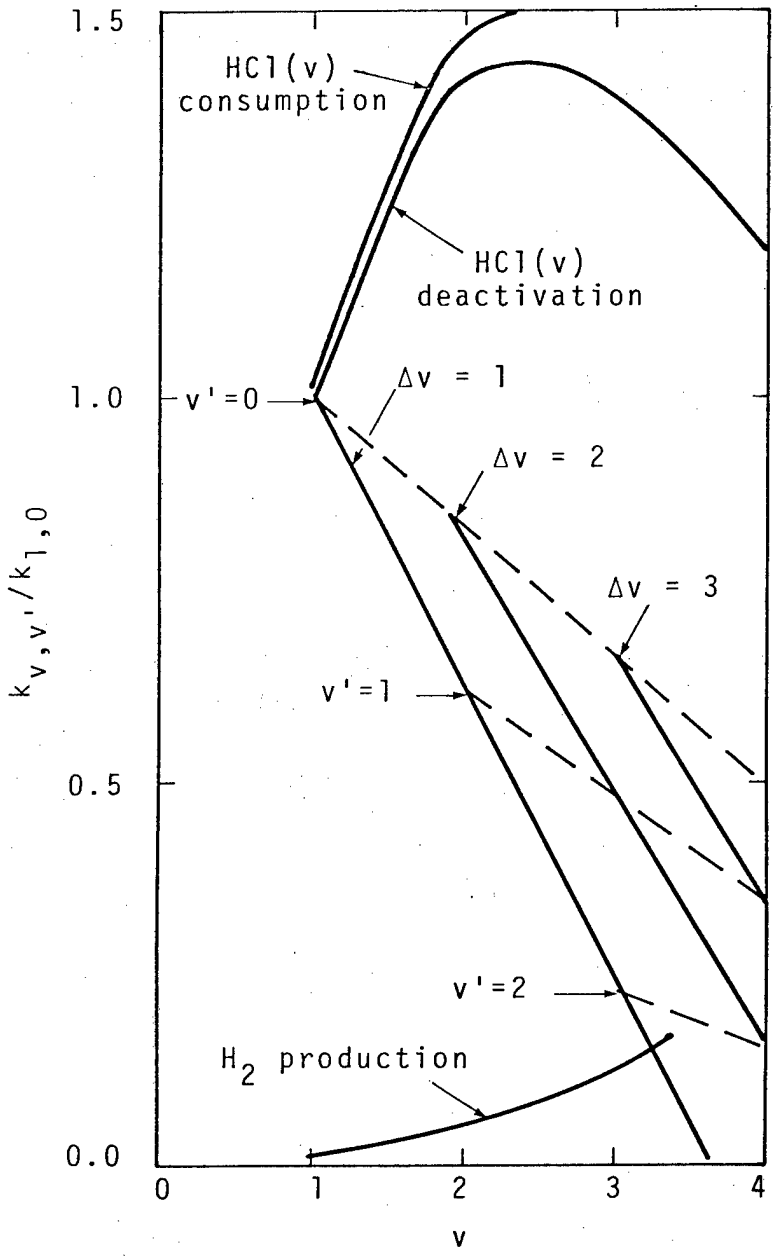

Figure 1. Relative Reaction and Deactivation Rates of HCl(v) by H atoms.

The computed room temperature rate constant of the H atom deactivation of the v=1 state of HCl, $(2.4 \pm .4) \times 10^{-11}$ cm^3/sec is in fair agreement with the measured rate constant, $(6.5 \pm 2.2) \times 10^{-12}$ cm^3/sec. Elimination of the atom exchange deactivation process reduces the rate constant from Wilkin's [3] value of 5.0×10^{-11} cm^3/sec; the remaining process is clearly the observed inelastic process.

The computed rate constant is overestimated because of inaccuracies in the empirical potential employed. The potential governing perpendicular H atom attack is not well specified by the data employed in determining this potential; therefore, sizeable errors may occur in that region. By continuity, the underestimate of the unknown potential for attack on the Cl end of the molecule cited above implies an underestimate for the poorly known region here. For this reason, the solid angle in which H atom attack is effective should be overestimated. Concommitantly, the rate of the deactivation reaction should be overestimated, but the fundamental physics of the process described is correct. Therefore, the trends predicted in this study– temperature and state dependences – are expected to be much more accurate than the magnitudes of the computed effects.

2.3. Results

The techniques described above have been applied to the rate of H atom collisional cooling of vibrationally excited HCl

$$H + HCl\ (v) \longrightarrow H + HCl\ (v')\quad (v' < v). \tag{4}$$

The temperature dependence of the $1 \longrightarrow 0$ process has been mapped from $300^{\circ}K$ to $1000^{\circ}K$, and the vibrational state dependence has been computed at $500^{\circ}K$.

The rates of the $1 \longrightarrow 0$ process given in Table I suggest a negative activation energy, -316 cal/mole. Within the accuracy of the present calculations, this rate constant

$$K_{1,0}(T) = A\,T^{\frac{1}{2}}\,e^{316/RT} \quad (300^{o} \leqslant T \leqslant 1000^{o}) \qquad (5)$$

is indistinguishable from the activationless process. Therefore, the assumption of that form introduces no significant error in modelling laser cavity chemistry.

The relative rates of the deactivation of the higher states are compared in Figure 1 and Table II. These results clearly show the inapplicability of the cannonical assumption that multiquantum collisional cooling is negligible. To the contrary, for this system the higher Δv processes are faster than those for lower Δv's. The rates of the detailed deactivation processes appear to decrease linearly with initial vibrational state up to v=3. (Beyond this value, contributions from the atom exchange process should alter the shapes of the curves given.)

The nature of the deactivation process is described by the mean change in translational energy associated with the deactivation. Figure 2 shows the $v \longrightarrow 0$ processes is essentially pure $v \longrightarrow T$ transfer. Transitions into the higher vibrational states leave increasing amounts of energy in diatomic rotation, but the process remains predominantly $v \longrightarrow T$ except for the $3 \longrightarrow 2$ process. Even in that case, half the energy is deposited in the translational mode.

The loss of HCl vibrational excitation to H atom collisions involves not only the deactivation processes described above, but also the reaction to form H_2

$$H + HCl \longrightarrow H_2 + Cl. \qquad (6)$$

Table I. Rate constants for H atom deactivation of HCl (v=1) between 300° and 1000°K.

T (°K)	$k_{1,0}(10^{-13}\,cm^3/sec)$
300	2.35 ± .39
500	2.38 ± .16
750	2.00 ± .46
1000	2.97 ± .12

Table II. Relative rate constants for H atom deactivation of HCl at 500°K

v	v'	$k_{v,v'}/k_{1,0}$
1	0	1.00
2	1	0.62
2	0	0.80
3	2	0.23
3	1	0.48
3	0	0.67

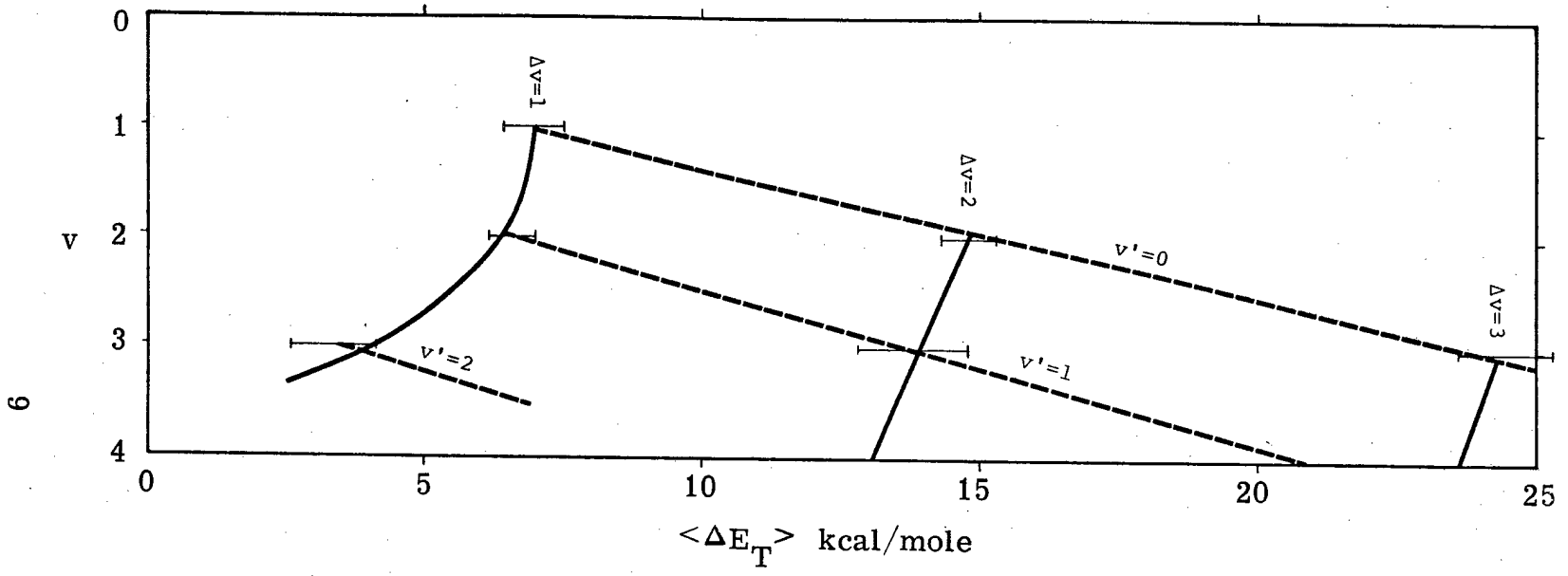

Figure 2. Mean Change in Translational Energy Accompanying H Atom Vibrational Deactivation of HCl at 500° K

Although slightly exothermic, this reaction is negligible under thermal conditions because it is inhibited by mass factors. The results in Figure 1 show the reaction rate rises exponentially with the HCl vibrational state to a value comparable to the deactivation processes for v=3. This leads to a systematic depopulation of the higher states, and therefore has a deleterious effect on laser performance.

State population is reduced by H atom deactivation to all lower states and by chemical reaction with those H atoms. The total rate of depopulation of the individual vibrational states is shown in Figure 1.

3.0 THE EFFECT OF INHOMOGENEOUS BROADENING AND CROSS RELAXATION ON HEL SYSTEM PERFORMANCE

A theoretical framework was provided in a previous report [10], to assess the importance of inhomogeneous broadening and cross relaxation on high energy laser system performance. In the present report the results of the previous work are extended, and the theory is applied to some additional laser systems of current interest.

3.1 Theory Review

The basic parameter f_{osc} is used to assess adequacy of the homogeneous line shape assumption for a laser oscillator [11, 12]. This parameter is defined as follows:

$$f_{osc} = \frac{F}{S}\left(\frac{\pi^2}{6}\right)\left(\frac{\Delta\nu_H}{\Delta\nu_D}\right)^3 \tag{7}$$

When f_{osc} is found to be greater than one, it may be safely assumed that the cross-relaxation rate and homogeneous line width combination is large enough so that the line may be assumed to be homogeneously broadened. If however f_{osc} is less than one, the homogeneous line assumption may not be valid. In the later case a more careful consideration of the particular laser system would be warranted to determine if a hole-burning type of gain saturation is limiting the output power of the laser.

Formulas for the various parameters occurring in equation (7) are repeated below because there are some typographical errors in the original report in the definition of these quantities. The cross-relaxation rate is assumed equal to the molecular collision rate and is given by

$$F = 4.6924 \times 10^{10}\,\sigma^2 p\left(\frac{1}{TM}\right)^{1/2} \qquad (\text{sec}^{-1}) \tag{8}$$

Here σ is the kinetic theory diameter in Å, p is the total cavity pressure in atmospheres, M is the reduced mass of the active molecule and perturber, and T is the Kelvin temperature. S is the stimulated emission rate per upper state molecule. The Lorentzian half-width is given by

$$\Delta\nu_H = 0.1766\ \sigma'^2 \left(\frac{1}{MT}\right)^{1/2} \qquad (cm^{-1}) \qquad (9)$$

where in the above σ' is the effective collision diameter for line broadening. The standard form of the Doppler half width is assumed (this equation was in error in the previous report):

$$\Delta\nu_D = 3.58 \times 10^{-7}\ \nu_0 \left(\frac{T}{m}\right)^{1/2} \qquad (cm^{-1}) \qquad (10)$$

In this expression, ν_0 is the frequency of the transition in wavenumber (cm^{-1}), and m is the mass of the active molecule in atomic mass units. Substitution of the above equation into equation (7) gives the following result.

$$f_{osc} = \frac{9.269 \times 10^{27} \sigma^2 \sigma'^6 m^{3/2} p}{S T^{7/2} M^2 \nu_0^3} \qquad (11)$$

In order to demonstrate the sensitivity of this equation to the various input parameters, we postulate a nominal pulsed HEL system. To construct such a system, we assume that it will be E-beam or E-beam-controlled discharge pumped, and operate at a total pressure of one atmosphere. We further assume that the active molecules are one percent of total and that one percent of the active molecules are inverted. Let us further assume that we have a duty cycle of 0.001 percent (i. e., 10 pps, 1 μsec pulse width). With these assumptions, the stimulated emission rate can be estimated by stipulating that the average power must be competitive with the DF HEL. Thus the

average output power must be equivalent to the 0.01 kw/cm^3 of DF. With those assumptions we obtain:

$$S \cong \frac{1.879 \times 10^{13}}{\nu_0} \tag{12}$$

Using the nominal values other parameters of Table III we obtain an equation for f_{osc} in our nominal pulsed HEL system.

$$f_{osc} = \frac{6.75 \times 10^{18}}{T^{7/2} \nu_0^{\ 2}} \tag{13}$$

The resulting f_{osc} values as a function of wavenumber and temperature are shown in Figure 3. That figure rather clearly shows that the shorter wavelength systems are much more susceptible to possible hole burning and subsequent gain saturation than are the infrared laser systems.

3.2 Application to Specific Systems

In the current period, we have investigated a number of other laser systems which are of current interest. Equation 11 can be used to predict the f_{osc} directly for a number of laser systems. The principal difficulty with this equation is obtaining a reasonable value of the stimulated emission rate per excited molecule. Small scale experiments can be used to estimate this rate when such results are available. Such estimates were used in the preceding report to derive f_{osc} values for a number of promising HEL systems. In the present period, we have considered a broad range of laser systems. The parameters used and the resulting f_{osc} values are shown in Table III. In determining the pulsed stimulated emission rate, a one pulse per second repetition rate at the indicated pulse width (w) has been

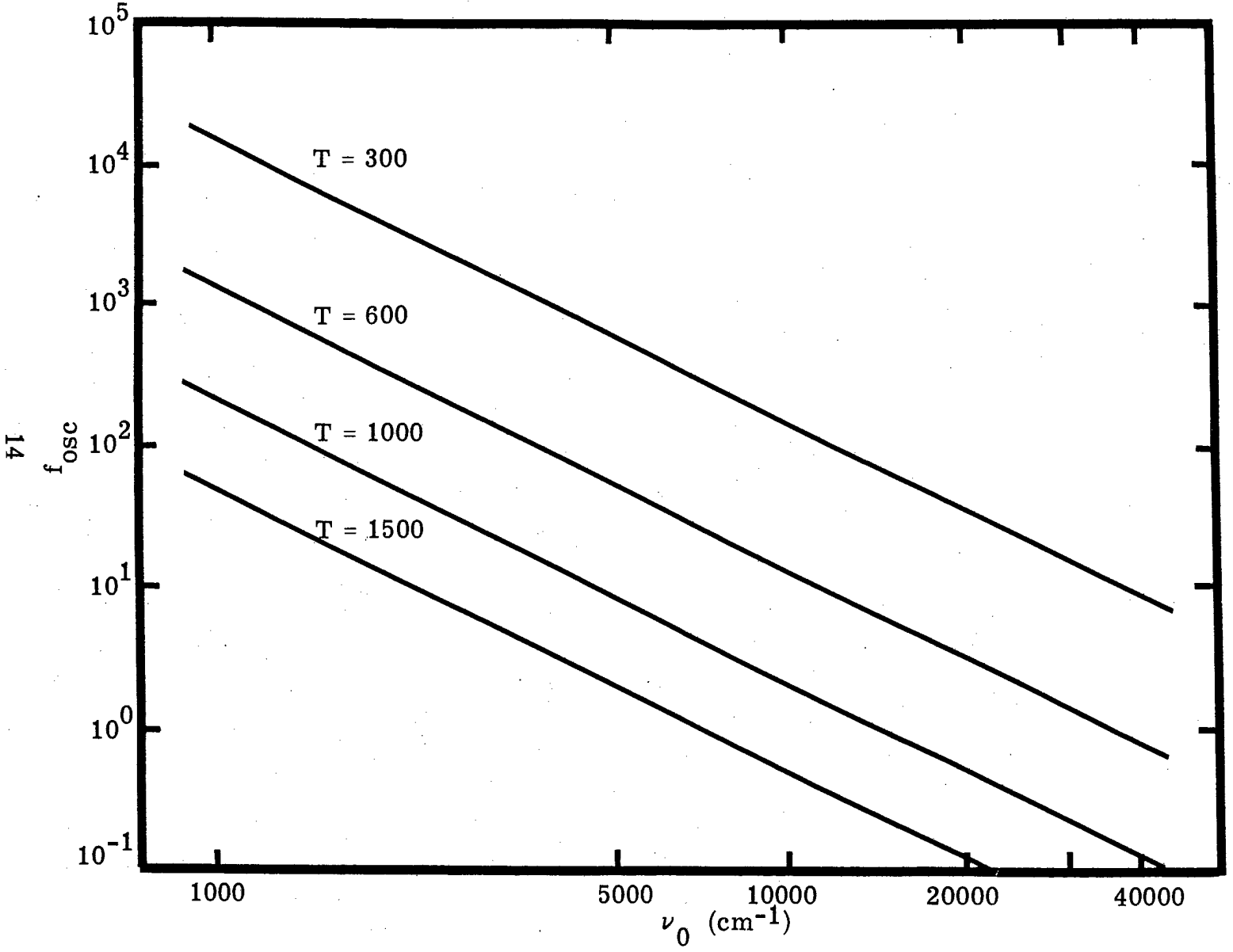

Figure 3. Homogeneous Broadening Parameter f_{osc} for a Nominal Pulsed Laser System

Table III

Evaluation of the Homogeneous Broadening Parameter f_{osc} for Various HEL Systems*

Parameter	Nominal Pulsed	Na_2[15]	K_2[14]	KrF[16]	HCl[1]
σ(Å)	3.0	3.0	3.0	3.0	3.0
σ'(Å)	3.0	3.0	3.0	3.0	4.4
m (Au) - Active	100	46	78	103	36
m (Au) - Diluent	28	4	131	40	2
M (Au)	21.9	3.68	48.9	28.8	1.9
ν_0 (cm^{-1})	Variable	12500	8600	40000	2600
T (^oK)	Variable	1000	250	300	600
P (atm) cont.	n.a.	0.05	10	1	0.1
S (sec^{-1}) cont.	n.a.	4.140×10^4	3.990×10^4	8580	1.320×10^5
$f_{osc,\ cont.}$	n.a.	2.740×10^4	2.794×10^7	2.980×10^5	2.951×10^8
P (atm) pulsed	1.0	0.05	10	1	
w (μ sec)	1	100	100	100	
S (sec^{-1}) pulsed	$1.879 \times 10^{13}/\nu_0$	9.140×10^8	3.990×10^4	8.580×10^7	
f_{osc}, pulsed	Figure 1	2.740×10^0	2.794×10^3	2.980×10^1	

* The parameters are estimates intended to be representative of a potential HEL system of the type indicated, although such a system may not currently exist.

assumed. The individual systems and the detailed results are discussed in the following paragraphs.

K_2 and Na_2 are both members of a class of proposed alkali-metal dimer laser systems. Such systems have been proposed by York and Gallagher [13] as efficient E-beam or discharged pumped systems. The K_2 system parameters given in Table III, are similar to those of a system where gain, although not lasing, has been measured by Palmer [14] in a self-sustained discharge laser configuration. As may be seen, the f_{osc} parameter is fairly large for this system and thus gain saturation does not appear to be a problem. This result should be typical of the high pressure (1 to 10 atmospheres) alkali-metal dimer systems.

The parameters chosen for the Na_2 system are representative of a low pressure alkali-dimer system. This type of laser is probably less adaptable to high power operation than the high pressure system, however Na_2 has been lased in a low pressure system with optical pumping [15]. It may be seen that when we assume HEL pulsed system operation the f_{osc} value approaches one. This indicates that some hole burning may take place in such a system. Whether this is an important effect will depend on the detailed operation of a specific laser.

The third laser system considered was a KrF laser. This laser is one of a class of recently demonstrated rare-gas mono-halide systems. In these systems an E-beam or E-beam sustained discharge is used to excite the rare gas atom. This excited rare gas atom behaves very much like an alkali-metal since it now has one electron in its outer shell. Thus the alkali-like rare-gas reacts readily with a halide to form a strongly bound ionic molecule in an excited state. The lasing transition is from the strongly bound excited state to a

weakly-bound or dissociative-ground state. Thus an inversion is easily produced. It may be seen from the table, that with our assumed parameters the pulsed high energy KrF laser system may be susceptible to gain saturation. In fact, since it appears that the laser may have a much shorter pulse width than has been assumed in our calculation [16]; inhomogeneous broadening may be a serious problem for a high power laser. However, the low power laser described in reference 16 does not show this. If inhomogeneous broadening were to occur for a high power mono-halide laser, it might be a serious problem since the short (20 nsec) spontaneous emission lifetime of the upper state provides a fast deactivation channel.

The final system considered in the present period is the proposed HCl non-reacting mixing laser [1]. In that laser, the HCl would be pumped by vibrational energy transfer from high temperature H_2. The resulting f_{osc} parameter for this laser clearly shows that the laser line may be considered totally homogeneous here. Thus, this laser is similar to the other infrared lasers considered in the earlier report, where the cross-relaxation rate is more than adequate to compensate for the fact that the homogeneous Lorentz widths are less than the inhomogeneous Doppler widths.

In the previous report a number of other potential HEL systems were also considered. The parameters used and the resulting f_{osc} values are given in Table IV. The complete table has been reproduced here, since a number of minor errors occurred in the previous publication. The final results, however are essentially the same as previously reported and the conclusions of that report are unchanged.

3.3 Conclusion

In this period, we have used the results of a modified rate equation theory, to assess the importance of inhomogeneous broadening and

Table IV

Previously Evaluated Homogeneous Broadening Parameters, f_{osc}, for Six Potential HEL Systems* [10]

Parameters	CO_2	DF	Xe	I	NaAr	BaO
σ(Å)	3.0	3.1	3.0	3.0	3.0	3.0
σ'(Å)	3.0	4.4	3.0	3.0	3.0	3.0
m (au) - Active	44	21	131	127	63	153
m (au) - Diluent	28	4	131	28	40	40
M (au)	17.1	3.36	65.5	22.9	24.5	31.7
ν_0 (cm^{-1})	940	2600	2949	7600	16500	16000
T (^oK)	500	600	500	500	1000	1500
P (atm) cont.	0.5	0.005	5.260×10^{-5}	.0037	10.	0.005
S (sec^{-1}) cont.	3.640×10^5	9.710×10^4	1.160×10^5	4.530×10^4	2.080×10^4	2.150×10^4
$f_{osc,\ cont.}$	2.592×10^7	3.051×10^6	1.344×10^2	1.105×10^4	1.715×10^5	4.975×10^1
P (atm) pulsed	0.5	1.0		0.0037	10.	0.005
w (μ sec)	50	10		100	100	100
S (sec^{-1}) pulsed	7.280×10^9	1.320×10^{10}		4.530×10^8	2.080×10^8	2.150×10^8
f_{osc}, pulsed	1.796×10^3	4.490×10^3		1.105×10^0	1.715×10^1	4.975×10^{-3}

* The parameters are estimates intended to be representative of potential HEL systems, although such systems may not currently exist.

cross relaxation on the operation of high energy laser systems. As a result of this work it is clear that typical HEL's which operate in the infrared have a sufficiently fast cross-relaxation rate to insure that the commonly used homogeneous line assumptions are valid. On the other hand, it appears that the inhomogeneous broadening of short wavelength pulsed laser systems may cause performance limitation under certain cavity conditions. Thus if high power visible lasers are constructed, the cavity conditions should be tailored to insure sufficient cross-relaxation rate so that the maximum energy may be efficiently extracted from the cavity.

4.0 ALKALI-NOBLE GAS LASER INVESTIGATION

In the present report, the NaAr molecule has been chosen as prototypical of the alkali-noble laser molecules. Here we present the results of an extensive ab initio and semi-empirical study of the potential functions, transition moment and spectral gain of this molecular system. The present results indicate that the bound $A^2\pi$ excited state results mainly from an ion-induced dipole interaction but with possible contribution from Van der Waals forces. The transition moment has also been calculated for the $A^2\pi$ to $X^2\Sigma$ laser transition. This calculation indicates that the transition moment variation with internuclear distance has a significant effect on the gain of the medium. Finally gain calculations are given for this system and extrapolation to other Na-noble gas systems is discussed.

4.1 Potential Curve Calculations

The important potential curves for the alkali-noble laser systems are the repulsive $X^2\Sigma$ ground state and the weakly bound $A^2\pi$ first excited state. Empirical scattering measurements have given approximate constants [17] and shapes for the ground states of these systems; however only recently have excited state potential curves become available [18]. A series of semi-empirical calculations have been published by Baylis [19] and Pascale and Vanderplanque [20] for the alkali-noble system. However these have consistently predicted excited state well depths less than half the values determined experimentally.

4.2 Upper Laser Level $A^2\pi$ State

The bound nature of alkali-noble excimers have long been assumed to be due principally to the attractive Van der Waals forces which are known to be important in long range ground state interactions between alkali and noble gas atoms. For example, the Baylis theory which does

explain greater than fifty percent of the well depth for most alkali-noble systems is based on the extrapolation of the Van der Waals attractive forces to the excited molecular states. Thus, in order to calculate more accurately the configuration interaction energies, including Van der Waals' contribution of the $A^2\pi$ state of NaAr, an extensive ab initio calculation was carried out.

4.2.1 $A^2\pi$ Configuration Interaction Results

In the NaAr Configuration Interaction (CI) calculation, we have followed a MC-SCF variational method previously used by Hirchfelder [21] and Das [22]. In this approach, a nominal size basis set is used to determine the configuration interaction energies between the principal Hartree-Fock (HF) configuration and the dispersion and other configurations which are expected to give significant attractive force contributions. It should be emphasized however, that only the CI potential contributions have been calculated here, since the basis set used is not large enough to predict the total interaction energy of the state accurately. The basis set and configurations used are listed in Tables V and VI. From Table V, it can be seen that a number of configurations which were omitted from our previous report [10] because of certain limitations of the computer codes have been included here through use of an alternate program. * The results of this calculation are given in Table VII. The $3p_{Na} - 3s_{Ar}$ results are omitted here, because in the MC-SCF itteration these configurations became identical with configurations contained in the $3p_{Na} - 3p_{Ar}$ group.

It is useful to analyse these results in terms of the expected C_6/R^6 dependence of the dispersion energy and the expected C_4/R^4

---

* We have recently been informed that these limitations have since been removed.

Table V.

Dominant Configurations Used in the Calculation of the $A\,^2\Pi$ State of NaAr

Description	Configurations $(Core_{Na}\ Core_{Ar})$ X	No. of Vector Couplings
Hartree-Fock	$3p\pi_{Na}(3s\sigma^2 3p\sigma^2 3p\pi^4)_{Ar}$	1
$(3p_{Na}, 3p_{Ar})$	$3s\sigma_{Na}\ 3d\pi_{Na}(3s\sigma^2 3p\sigma^2 3p\pi^3 3d\pi)_{Ar}$	4, 2*
	$3d\delta_{Na}(3s\sigma^2 3p\sigma^2 3p\pi^3 3d\sigma)_{Ar}$	2+
	$3d\sigma_{Na}(3s\sigma^2 3p\sigma^2 3p\pi^3 3d\sigma)_{Ar}$	2
	$3d\sigma_{Na}(3s\sigma^2 3p\sigma^2 3p\pi^3 3d\delta)_{Ar}$	2+
	$3d\delta_{Na}(3s\sigma^2 3p\sigma^2 3p\pi^3 3d\delta)_{Ar}$	2, 2*
	$3d\delta_{Na}(3s\sigma^2 3p\sigma 3d\pi 3p\pi^4)_{Ar}$	2+
	$3d\sigma_{Na}(3s\sigma^2 3p\sigma 3d\pi 3p\pi^4)_{Ar}$	2
	$3d\pi_{Na}(3s\sigma^2 3p\sigma 3d\sigma 3p\pi^4)_{Ar}$	2
$(3p_{Na}, 3s_{Ar})$	$3d\pi_{Na}(3s\sigma 3p\sigma^2 4p\sigma 3p\pi^4)_{Ar}$	2
	$3d\delta_{Na}(3s\sigma 3p\sigma^2 4p\pi 3p\pi^4)_{Ar}$	2+
	$3d\sigma_{Na}(3s\sigma 3p\sigma^2 4p\pi 3p\pi^4)_{Ar}$	2
Overlap-Charge-Transfer	$3p\pi^2_{Na}(3s\sigma^2 3p\sigma 4p\sigma 3p\pi^3)_{Ar}$	7
	$3p\pi^2_{Na}(3s\sigma^2 3p\sigma 3d\sigma 3p\pi^3)_{Ar}$	7

* These omitted configurations will contribute only to dispersive terms of higher order than the C_8 term.

\+ The contributions from these configurations were calculated using MC-SCF codes provided by Dr. J. Hinze of the University of Chicago.

Table VI.
Basis Set Used for the Calculation of the $A\,^2\pi$ State of NaAr

nl	σ-Set Exponent	nl	π-Set Exponent	nl	δ-Set Exponent
Na 10	10.6259[a]	Na 21	3.4009	Na 32	0.75
20	3.2857[a]	31	0.8592	42	0.75
30	1.24[a]	31	0.5292	43	0.8592
30	0.75[a]	32	0.75	43	0.5292
21	3.4009[a]	42	0.75		
31	0.8592[b]	43	0.8592		
31	0.5292[b]	43	0.5292		
32	0.75[c]				
42	0.75[c]				
43	0.8592[c]				
43	0.5292[c]				
Ar 10	17.5057[a]	Ar 21	7.0041	Ar 32	2.893
20	6.1152[a]	31	2.893	32	1.605
30	2.5856[a]	31	1.605	42	2.893
21	7.0041[a]	41	2.5856	42	1.605
31	2.893[b]	32	2.893	43	2.2547
31	1.605[b]	32	1.605		
41	2.5856[c]	42	2.893		
32	2.893[c]	42	1.605		
32	1.605[c]	43	2.2547		
42	2.893[c]				
42	1.605[c]				
43	2.2547[c]				

a. Taken from either the minimal or nominal basis set for Na or Ar as listed in the BISON program of Argonne National Laboratory.
b. Taken from the HF calculation for Na-Ar by Janis and Wahl [25].
c. Chosen for the excitations as prescribed in Ref. 22.

Table VII.

Results of Configuration Interaction Calculation for the $A\,^2\pi$ State of NaAr

Internuclear Separation (Bohr)	$3p_{Na} - 3p_{Ar}$ (Hartree x 10^3)	Charge - Transfer (Hartree x 10^3)	V_{CI} (Hartree)
5.5	-1.966	-0.265	-2.321
6.0	-1.604	-0.198	-1.802
7.0	-1.005	-0.114	-1.119
10.0	-0.224	-0.012	-0.236

dependence for the ion-induced dipole potential. The C_6 coefficient determined from the CI results is shown as a function of R in Figure 4. The ten bohr $C_6(R)$ value of 236 in atomic units is slightly larger than the calculated asymptotic value of 190 for the ground state of NaAr [23]. The expected decrease of the $C_6(R)$ coefficients as internuclear distance decreases is similar to the results of previous calculations on similar systems [24].

The CI energy contribution has also been used to determine the $C_4(R)$ coefficient expected with an ion-induced dipole interaction. The results of such a calculation are given in Figure 4. From that figure it is clear that the $C_4(R)$ analysis gives a much flatter R dependence, leading to the conclusion that the principal attractive forces here are not dispersion forces but rather the ion-induced dipole attraction.

4.2.2 $A\,^2\pi$ Hartree-Fock Potential

As discussed in our previous report, it was expected that the addition of the calculated CI potential to the large basis HF potential computed by Janis and Wahl [25] would provide an accurate representation of the NaAr $A\,^2\pi$ potential. However after a thorough examination of results obtained for the small basis HF configuration included in the current MC-SCF calculation, it became apparent that an ion-induced dipole interaction is also important for the HF potential. In fact, in contrast to the earlier HF results, our HF results show significant binding due to a mixture between the $A\,^2\pi$ and higher $^2\pi$ states. The dominant effect seen is the polarization of the Na $3p\pi$ orbital away from the incoming Ar atom through orbital mixing with the Na $4d\pi$ orbital. Mixing is also observed with the $3p\pi$ and $4p\pi$ Ar orbitals. Thus the valence orbital is taking on the character of a united atom orbital and the Na atom begins to take on the character of the Na^+

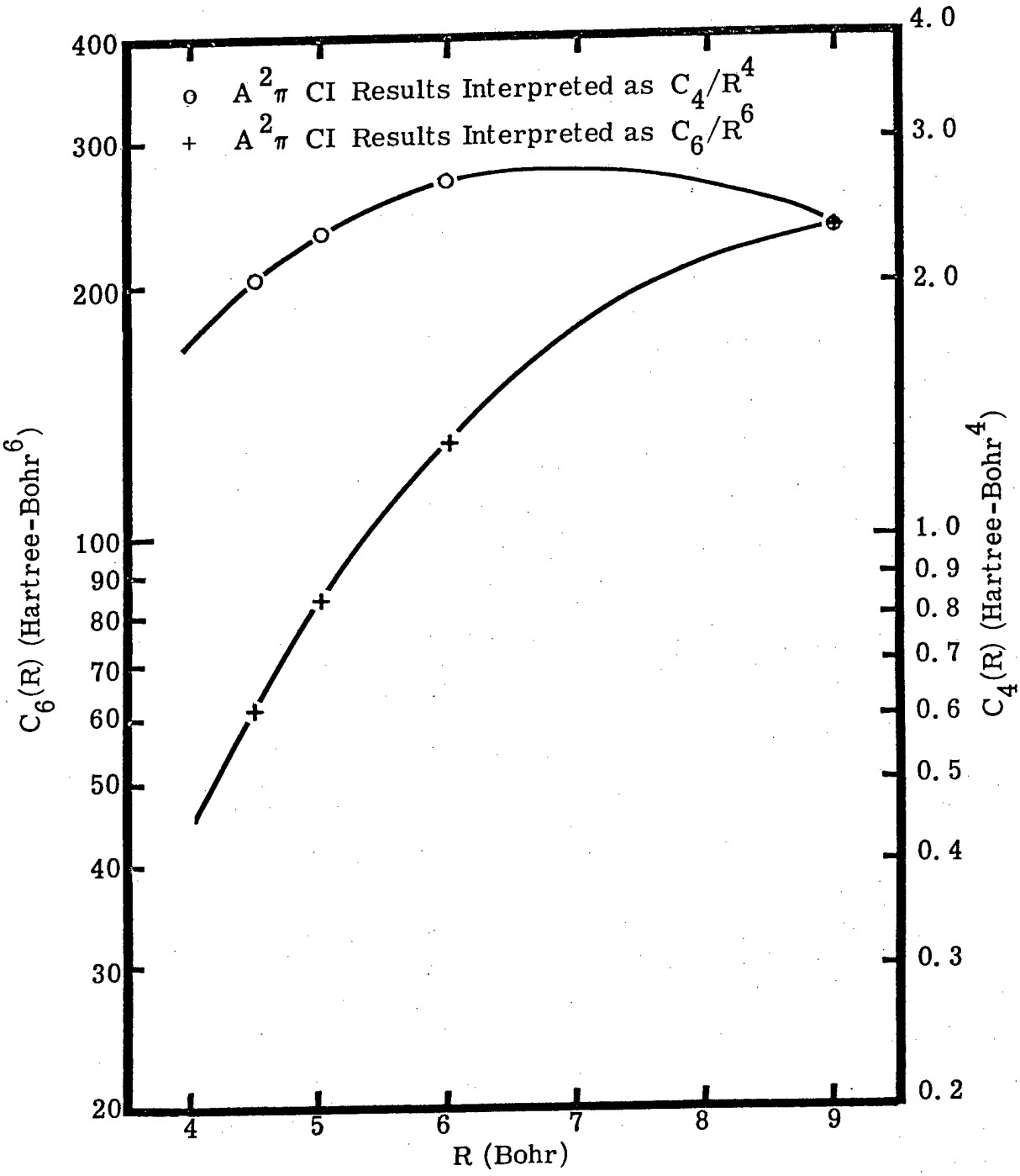

Figure 4. C_4(R) and C_6(R) Coefficients Determined by the CI Calculations for the $A^2\pi$ State of NaAr

ion from the perspective of the Ar atom. The previous HF calculation did not show this binding effect because neither the important $4p\pi$ nor the $4d\pi$ orbitals were included in the basis set used there. On the other hand, the basis set used in the present MC-SCF calculation is simply too small to give an accurate HF potential. Neither of these HF potentials now appears to be an accurate representation of the true $A\,^2\pi$ state HF potential in light of our present understanding of the physics, but the large basis HF potential can conveniently be used with the experimental results to get a better understanding of the importance of the attractive potential effects.

4.2.3 NaAr $A\,^2\pi$ - Total Attractive Potential

The attractive potential for intermediate internuclear separations is conveniently obtained by substracting the HF energy from the experimental potential values of York [18]. When this is done and the results are analysed as C_4/R^4 or C_6/R^6 interactions, the C(R) curves of Figure 5 are obtained. Again, from that figure it is apparent that the C_4 interpretation gives the more constant value of the force constant.

It seems clear from our CI results and the semi-empirical analysis given above, that in the well region near the potential minimum the principal bonding force results from an ion-induced dipole effects. The turn over of the $C_4(R)$ in Figure 4, beyond 8 bohrs indicates that at that point the C_6 dispersion forces probably are becoming important while the C_4 ion-induced dipole forces are becoming less significant. The calculated CI contribution and the total potential of the $A\,^2\pi$ state is given in Figure 6 and Table VIII.

4.3 Lower Laser Level - NaAr $X\,^2\Sigma_{1/2}$ State

The $X\,^2\Sigma_{1/2}$ potential is important because the shape and relative position of this potential with respect to the excited state determines the peak laser gain wavelength. Two types of measurements are

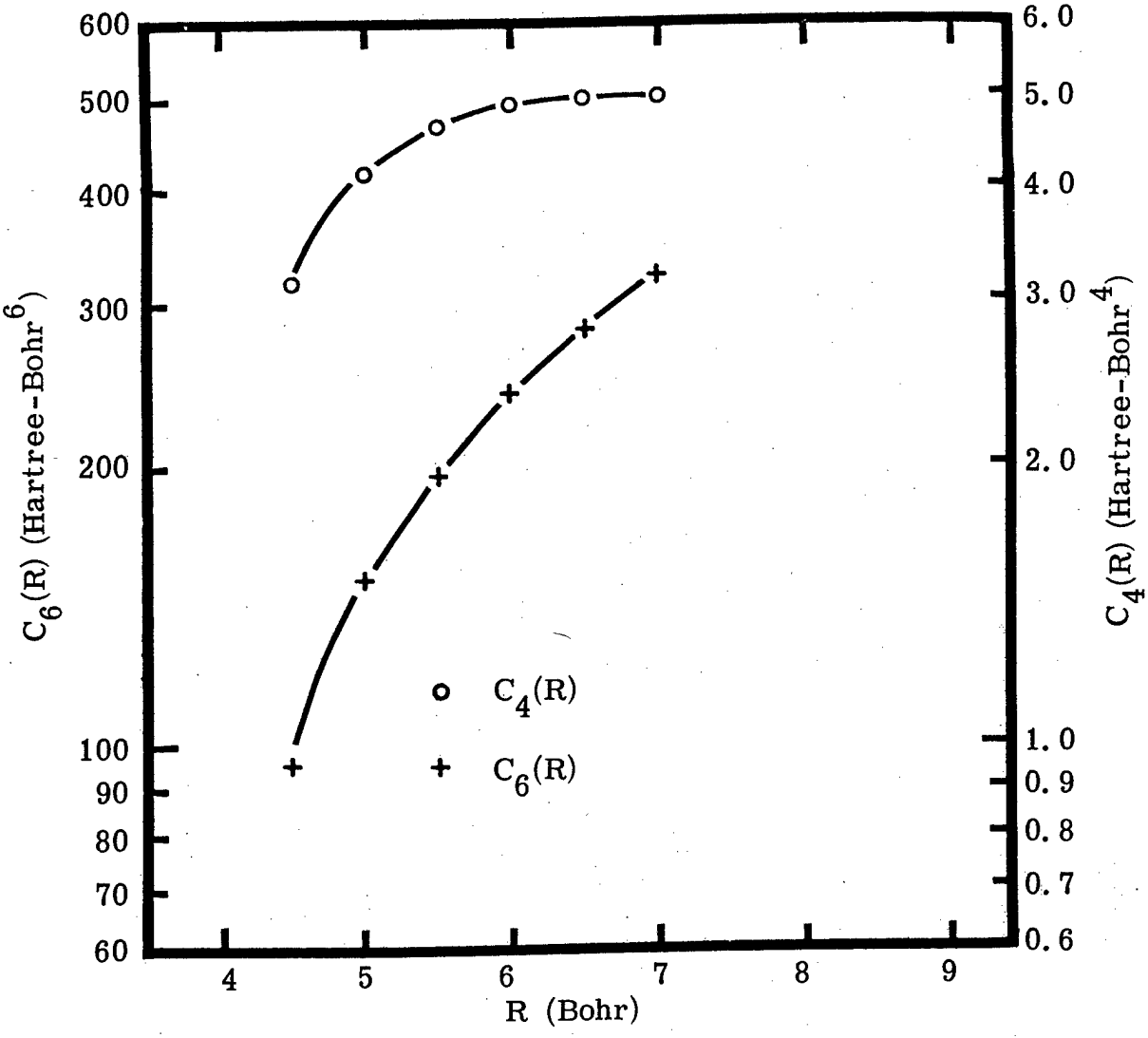

Figure 5. $C_4(R)$ and $C_6(R)$ Coefficients for the Total Attractive Portion of the $A\,^2\pi$ State of NaAr

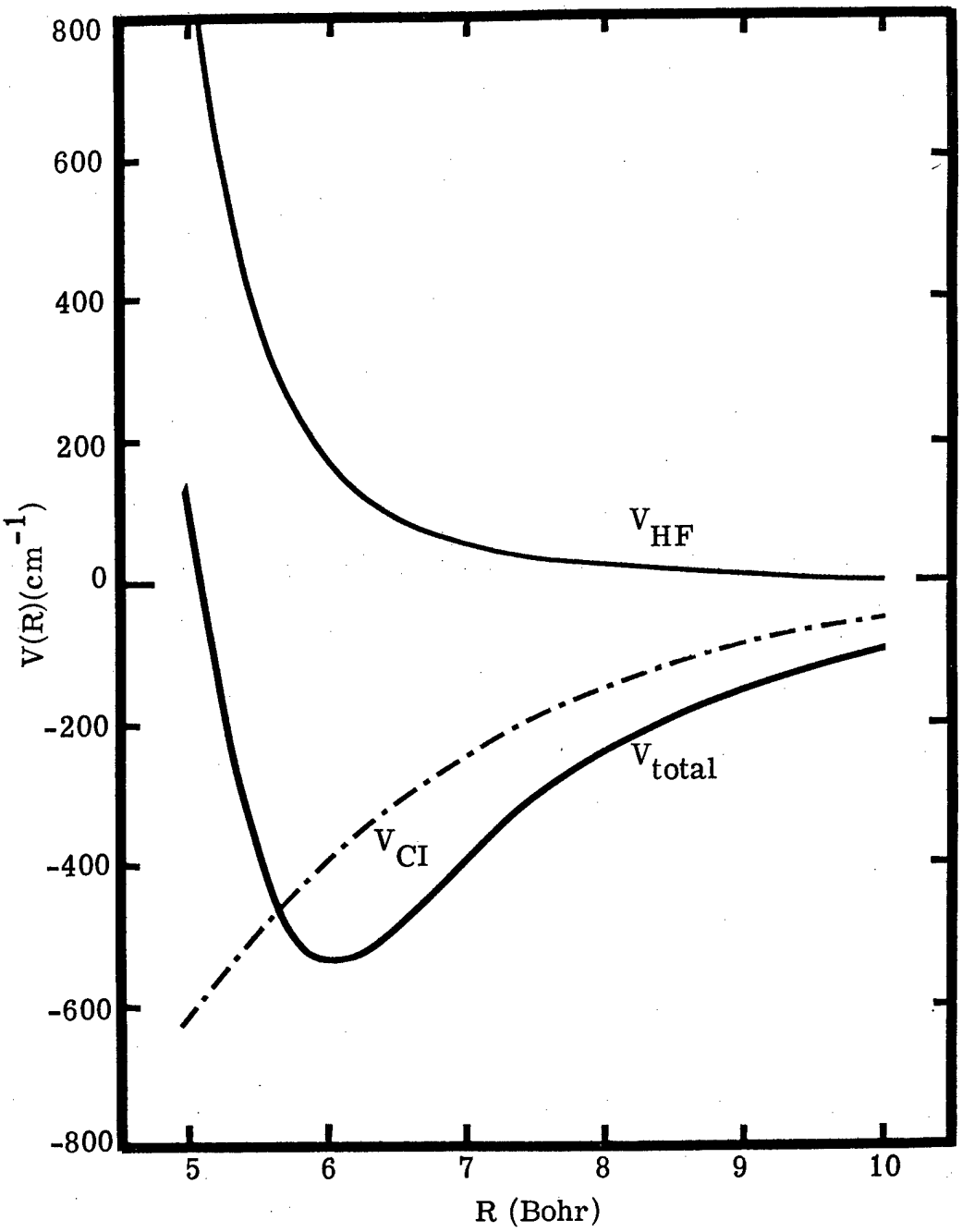

Figure 6. Contributions of Various Terms to the $A\,^2\pi$ Potential of NaAr

Table VIII. Various Contributions to the $A^2\pi$ Potential of NaAr

R(AU)	V_{HF}[25]	V_{CI}	V^*_{Att}	V_{total}		V_{exp}[18]
Bohr	Hartree x 10^3	Hartree x 10^3	Hartree x 10^3	Hartree x 10^3	cm^{-1}	cm^{-1}
5.0	4.35	-2.816		0.526	115	
5.5	1.69	-2.231	-3.461	-1.771	-389	-389
6.0	0.79	-1.802	-3.229	-2.439	-535	-517
6.5	0.42	-1.405	-2.626	-2.206	-484	-498
7.0	0.26	-1.119	-2.046	-1.786	-392	-395
7.5	0.17	-0.876	-1.579	-1.409	-309	-302
8.0	0.13	-0.687	-1.230	-1.100	-241	-238
8.5	0.07	-0.530		-0.886	-194	
9.0	0.05	-0.406		-0.695	-153	
9.5	0.02	-0.306		-0.559	-123	
10.0	-0.00	-0.236		-0.459	-100	

* Contains V_{CI} contributions.

Table IX. Various Contributions to the $X^2\Sigma$ Potential of NaAr

R	V_{HF}[25]	V_{disp}	V_{total}		V_{exp}[17]
Bohr	Hartree x 10^3	Hartree x 10^3	Hartree x 10^3	cm^{-1}	(cm^{-1})
5.0	13.19	-2.83	10.36	2274	2375
6.0	5.86	-1.72	4.14	909	795
7.0	2.70	-1.07	1.63	358	315
8.0	1.09	-0.64	0.45	99	142
9.0	0.40	-0.35	0.05	11	
10.0	0.07	-0.19	-0.12	-26	

available for this potential, but both have certain limitations. Scattering measurements results of Malerick and Cross [17] are interpreted as giving a C_6/R^6 repulsive potential with a value of the repulsive constant of 3.71 in atomic units. This however, must be treated as only an approximation to the true curve. The other experimental potential curve was determined by York [18] from pressure dependent emission measurements. The shape and position of this potential are not unambiguously determined by the fluorescence measurement since the analysis of those results requires that a starting radius to fix the potential position be taken from another measurement.

4.3.1 $X^2\Sigma_{1/2}$ Hartree-Fock Potential

The Hartree-Fock potential for the $X^2\Sigma_{1/2}$ state of NaAr has been calculated by Janis and Wahl [25] with the same basis set used for the $A^2\pi$ state. For this state, the ion-induced dipole effect should be negligible because of the symmetry of the $3p\sigma$ state. Thus we would expect the HF calculation to give an accurate representation of the single configuration energy. Of course, since configuration interaction is not included here, dispersion effects must be added to the HF results to give an accurate representation of the true molecular potential.

4.3.2 $X^2\Sigma_{1/2}$ Van der Waals Potential

The Van der Waals calculation for this state has not been completed; however, an approximate Van der Waals potential for this state can be determined through the use of HF results and the scattering measurement. The resulting $C_6(R)$ coefficient values from such a calculation are plotted in Figure 7. We have simply assumed the smooth curve indicated on that figure for the dispersion coefficient

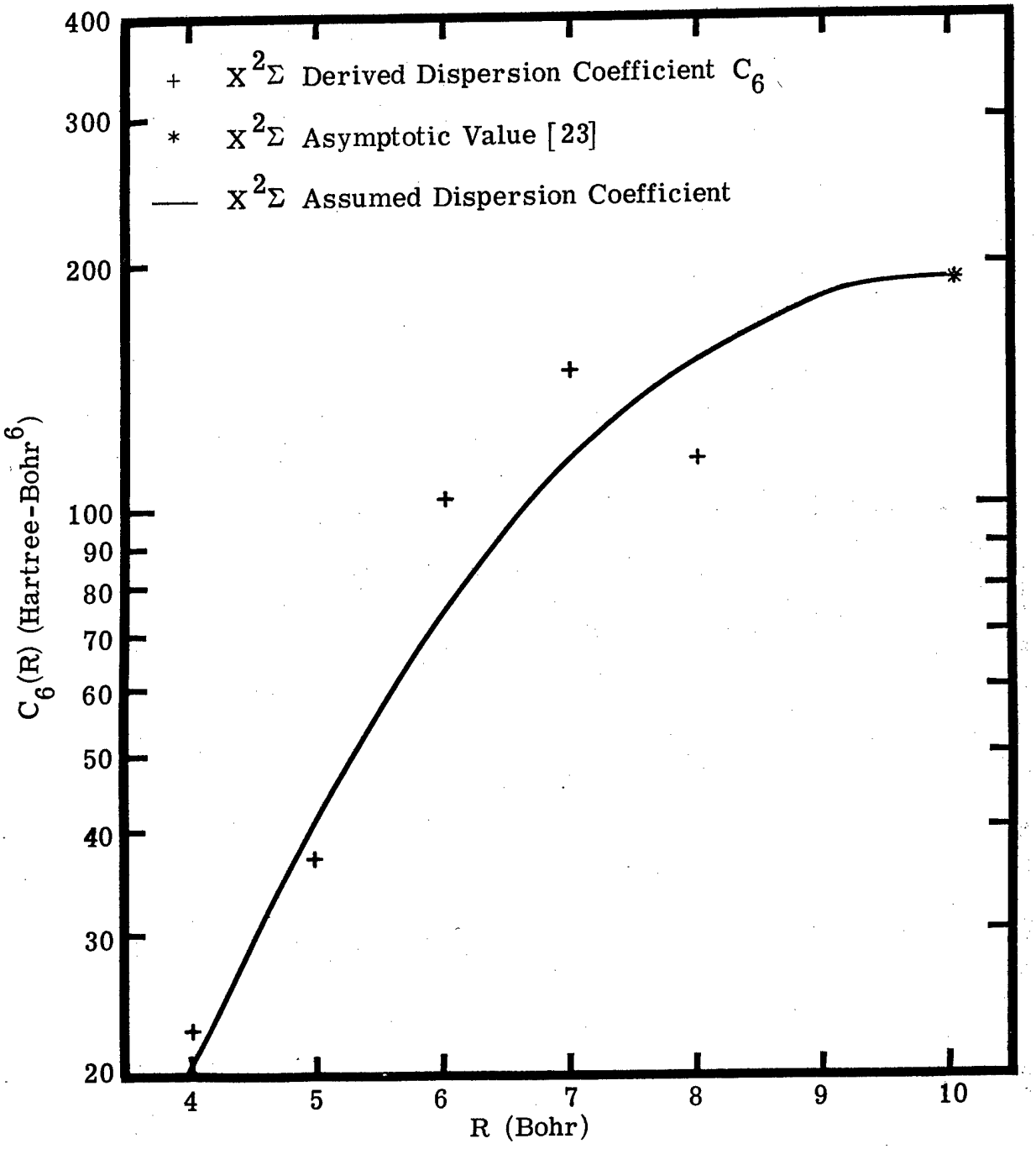

Figure 7. $C_6(R)$ Dispersion Coefficients Determined for the $X^2\Sigma$ State of NaAr

and combined the resulting dispersion potential with the HF potential of Janis to obtain the $X^2\Sigma$ potential given in Table IX and Figure 8. It can be seen from that figure that this potential is in reasonable agreement with the potential obtained by York [19].

4.4 Transition Moment Calculations

The dipole transition moment is also required for laser gain calculation. Earlier computations have assumed that the transition moment is independent of the internuclear separation [10, 26]. In the present study we have calculated the transition moment in the HF approximation with the wave functions determined by Janis and Wahl. From those wave functions, both the dipole length and dipole velocity transition moments forms were calculations with the use of an Argonne computer code [27]. The resulting oscillator strengths and transition moment values for NaAr are given in Table X. These results may be compared with the dipole length oscillator strength values of Table XI computed by Krauss, Maldonado and Wahl [27] for the similar NaHe molecule. The divergence between the f_l and f_v forms of the oscillator strength is disturbing, however, in light of the similarity between the f_l values for NaAr and NaHe, these f_l values might be preferred. The ion-induced dipole and the Van der Waals wave functions would also be expected to provide significant correction to the HF transition moment, so the values given here must be considered approximate.

4.5 NaAr Gain Calculation

Under the quasi-static theory assumption, the reduced laser gain is given by the following expression [28]:

$$g(\nu) = \frac{\lambda^2}{2} A_{ul}(\nu) \frac{g_u}{g_{fl}} \frac{R^2}{\left|\frac{d\nu}{dR}\right|} \left[\exp\left(- \frac{V'(R)}{kT} - \frac{h\nu_0}{kT_e} \right) - \exp\left(- \frac{V''(R)}{kT} \right) \right]$$

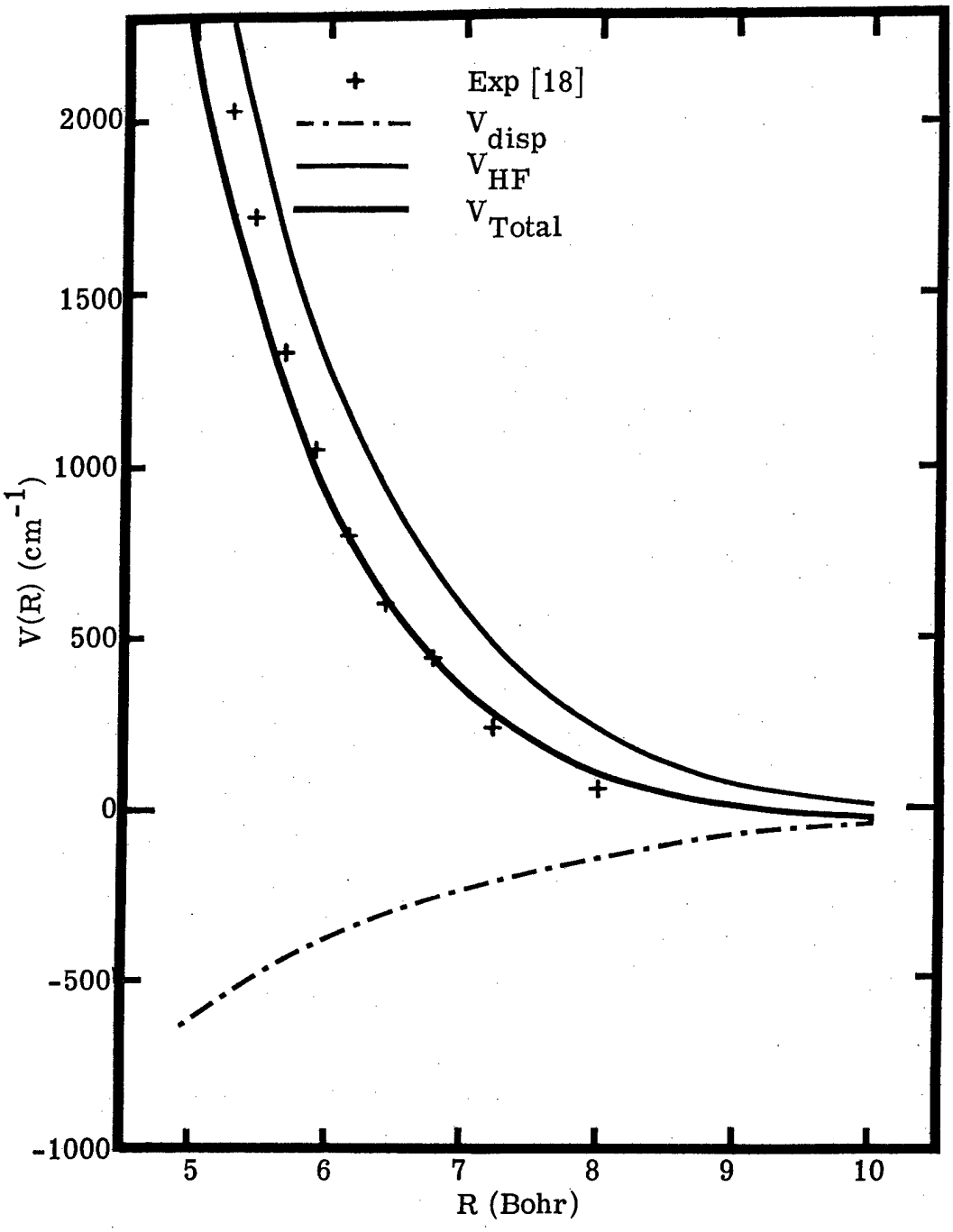

Figure 8. Contributions of Various Terms to the $X^2\Sigma$ Potential of NaAr

Table X.

Calculated Oscillator Strengths and Dipole Transition Moments for the $X\,^2\Sigma^+ - A\,^2\pi$ Transition of NaAr

Internuclear Separation R(bohr)	Oscillator Strength		Square of Transition Moment $\lvert\mu_{\pi\Sigma}\rvert^2$ (electron - bohr)^2	
	(dipole length) f_l	(dipole velocity) f_v	(from f_l)	(from f_v)
5.0	0.578	0.666	6.82	7.86
6.0	0.607	0.665	6.76	7.40
8.0	0.639	0.656	6.71	6.87
∞	Exp. f = 0.654		$\lvert\mu_{Na}\rvert^2$ = 6.35	

Table XI

Oscillator Strength and Dipole Transition Moment of NaHe [27] $X\,^2\Sigma - A\,^2\pi$

Internuclear Separation R(bohr)	Oscillator Strength (dipole length) f_l	Square of Transition Moment $\lvert\mu_{\pi\Sigma}\rvert^2$ (electron - bohr)^2
5.0	0.610	6.92
6.0	0.631	6.87
8.0	0.646	6.73
∞	0.649	6.72

* Calculated from the f_l given in reference [27].

The frequency of the transition is given by

$$\nu(R) = V'(R) - V''(R).$$

For the lower and upper state potentials V'' and V', lease square fits to the results given in Tables VIII and IX were used.

The Einstein coefficient is represented by the expression

$$A_{ul}(\nu) = A(\lambda_0) \left(\frac{\lambda_0}{\lambda}\right)^3 \frac{\mu_{\pi\Sigma}(R)^2}{\mu_{Na}^2}$$

where $\mu_{\pi\Sigma}(R)$ is fit to the results of Table X and μ_{Na} is the experimental oscillator strength for the Na D_2 transition. A value of $A(\lambda_0)$ of 6.667×10^7 sec^{-1} was used with λ_0 equal to 5890 Å. A translational temperature of 650^o K and an electronic temperature of 7000^o K have been assumed.

The resulting reduced gain, stimulated emission and absorption coefficients are given in Figures 9 and 10. In Figure 9, the constant value of the transition moment has been assumed. This leads to a peak gain of 1.24×10^{-39} cm^5 at 6640 Å. This wavelength corresponds to an inter-nuclear separation of 5.55 bohrs which is on the inner wall of the excited state potential. Figure 10 shows the range of results obtained with the two forms of the calculated, radius-dependent transition moment representations. The f_v form gives the largest peak gain value of 1.69×10^{-39} cm^5 almost 40% greater than the constant moment result.

4.6 Conclusion

A number of alkali-noble gas laser systems have been investigated theoretically. This investigation has indicated that the $A^2\pi$ excited bound state of the NaAr molecule is basically a Rydberg state where ion-induced dipole and Van der Waals forces both significantly contribute

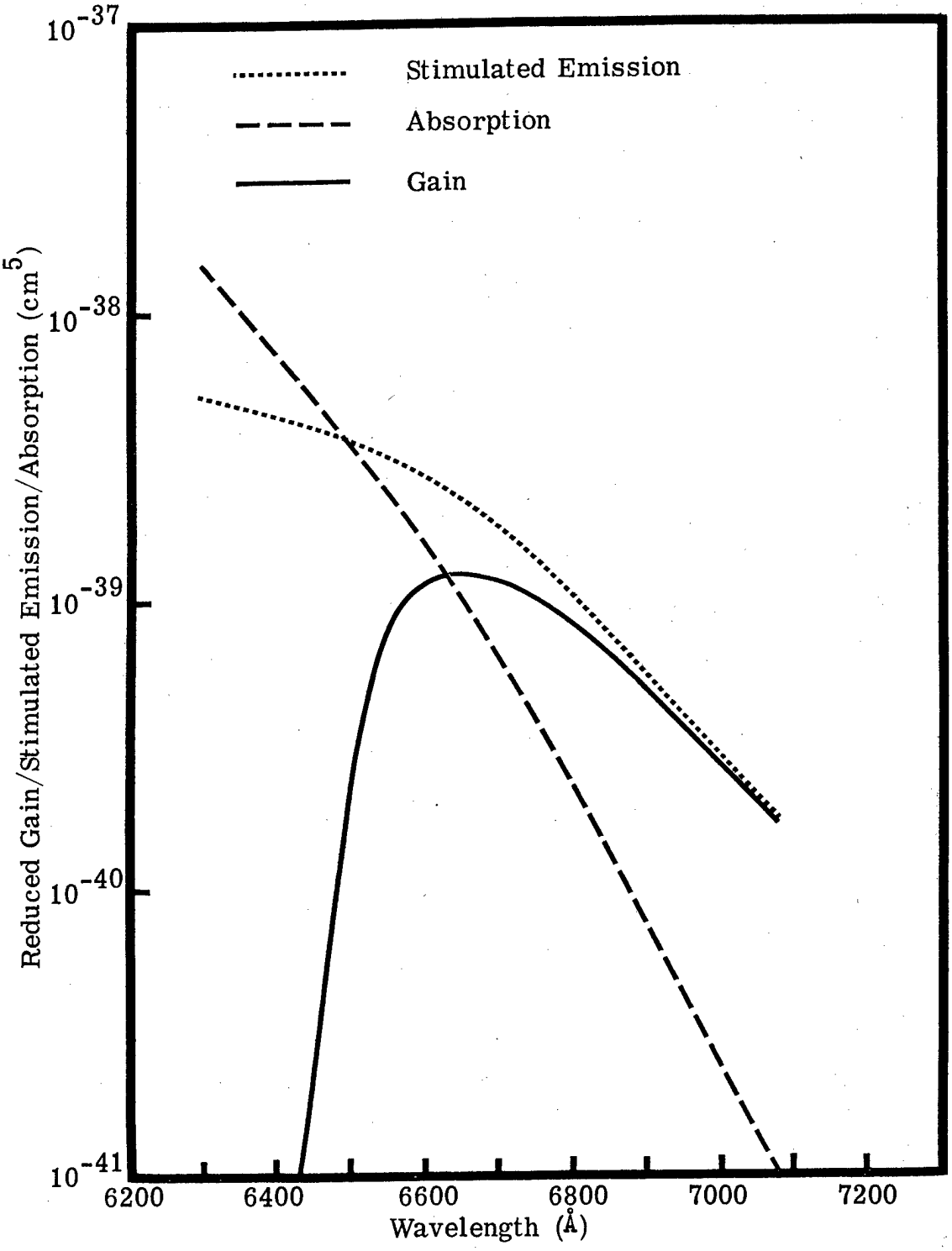

Figure 9. Reduced Gain, Stimulated Emission and Absorption for NaAr with a Constant Transition Moment

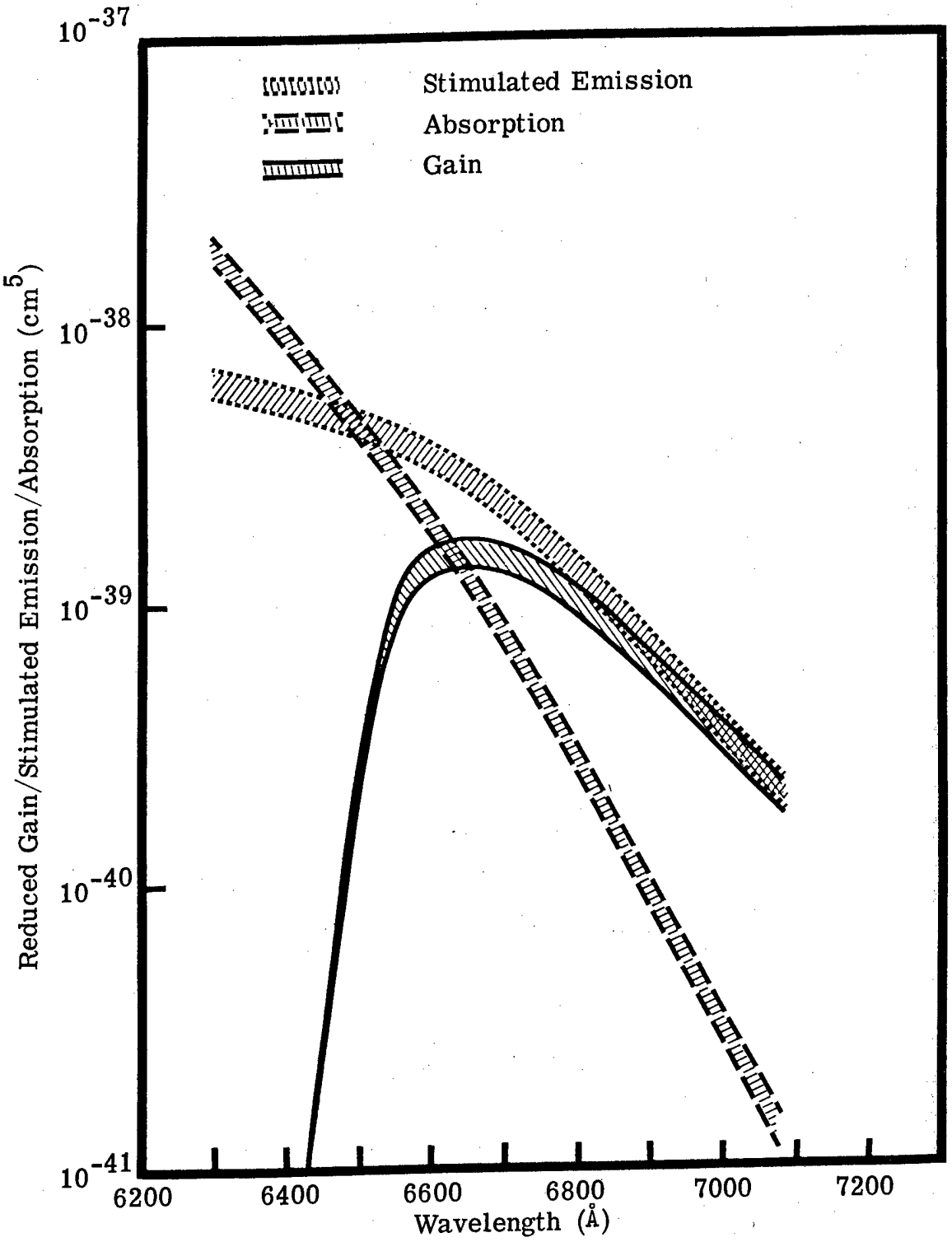

Figure 10. Reduced Gain, Stimulated Emission and Absorption for NaAr Calculated with a R-Dependent Transition Moment

to the binding. In the course of this investigation a number of theoretical gain calculations which can be used to predict the gain for actual laser media conditions have been performed. It has been shown that predicted variations of the transition moment can cause a significant change in the predicted gain in the NaAr system.

The current study indicates that ab initio molecular calculations are useful in obtaining information on the chemistry of alkali-noble molecule formation important for laser design. However, such calculations are expensive, and care must be exercised to limit the quantity of calculations, to include the minimum required to obtain the desired theoretical information. We find that the physical insight gained from ab initio calculations on intermediate size systems like NaAr is considerable, and that it can be applied with more confidence to interpret larger, similar molecules than can extrapolations from the more typical, small molecule ab initio results.

REFERENCES

1. R. L. Taylor, P. Lewis, J. D. Teare, R. Naismith and R. Cavalleri, Final Report for Phase I of the NRML Laser, ARC 47-5629, Atlantic Research Corp., Alexandria, VA (1975).

2. D. Arnoldi and J. Walfrum, Chem. Phys. Letters, 24, 234, (1974); Brown, Glass & Smith, ibid. to be published.

3. R. L. Wilkins, Vibrational Relaxation of HCl (v=1, 2, 3, 6) by H and Cl Atoms, Report SAMSO-TR-75-74.

4. A. Persky & F. S. Klein, J. Chem. Phys., 44, 3617 (1966).

5. F. O. Ellison, J. Am. Chem. Soc., 85, 3540 (1963); C. W. Wilson, Jr., J. Chem. Phys., 62, 4842 (1974) and references therein.

6. J. C. Tully, J. Chem. Phys., 58, 1396 (1973).

7. C. F. Bender, B. J. Garrison & H. F. Schaefer III, J. Chem. Phys., 62, 1188 (1975).

8. C. A. Parr & D. G. Truhlar, J. Chem. Phys., 75, 1844 (1971).

9. J. C. Polanyi and co-workers, private communication (1972).

10. T. S. Chang, et. al., Inhomogeneous Broadening Effects and Gain Calculations for Potential Short Wavelength Laser Systems, Technical Report SAI-75-003-AA, Science Applications, Inc., May 1975.

11. A. Y. Cabezas and R. P. Treat, J. Appl. Phys., Vol. 37, p. 3556. 1964.

12. E. R. Peressini and G. L. Linford, J. Quantum. Elect., Vol. QE-4, p. 657, 1968.

13. G. York and A. Gallagher, High Power Gas Lasers Based on Alkali-Dimer A-X Band Radiation, JILA Report 114, Univ. of Colorado, Boulder, CO, 1974.

14. A. J. Palmer, Excimer Lasers, Technical Report on Contract N00014-75-C-0081, June 1975.

15. R. L. Byer, Stanford University, Private Communication.

16. J. A. Mangano and J. H. Jacob, Appl. Phys. Letter, Vol. 27, p. 495, 1975.

17. C. J. Malerick and R. J. Cross, J. Chem. Phys., 52, 386 (1970) and references therein.

18. G. York, et. al., J. Chem. Phys., 63, 1052, 1975.

19. W. E. Baylis, J. Chem. Phys., 51, 2665, 1969.

20. J. Pascale and J. Vandeplanque, J. Chem. Phys., 60, 2278 (1974).

21. J. O. Hirschfelder and W. J. Meath, Adv. Chem. Phys., XII, 3, 1967.

22. G. Das and A. C. Wahl, Phys. Rev. A, 4, 825, 1971.

23. A. Dalgarno, Adv. in Chem. Phys., XII, 164, 1967.

24. Y. S. Kim and R. G. Gordon, J. Chem. Phys., 61, 1, 1974.

25. T. Janis and A. C. Wahl, to be submitted to J. Chem. Phys.

26. A. V. Phelps, "Excimer Lasers and Spectral Line Broadening," Second International Conference on Spectral Lines, Aug. 1974, Eugene, OR.

27. M. Krauss, P. Maldonado and A. C. Wahl, J. Chem. Phys., 54, 4944, 1971.

28. R. E. Meredith, et. al., Investigations in Support of High Energy Laser Technology, Semi-Annual Technical Report SAI-73-004-AA, Science Applications, Inc., Ann Arbor, MI, December 1973.

DISTRIBUTION LIST

Defense Advanced Research Project Agency
Attn: Director, Laser Division

ODDR&E, Pentagon
Attn: Ass't Director
(Space and Advanced Systems)

US Arms Control and Disarmament Agency
Attn: Dr. Charles Henkin

US Atomic Energy Commission
Division of Military Application
Attn: Dr. Lawrence E. Killion

National Aeronautics and Space Administration
Code RR, ROB 10B

National Aeronautics and Space Administration
Lewis Research Center
Attn: Dr. John W. Dunning, Jr.
(Aerospace Res. Engineer)

National Aeronautics and Space Administration
Ames Research Center
Attn: Mr. Robert L. McKenzie
Dr. Kenneth W. Billman

National Security Agency
Attn: Mr. Richard C. Floss A763
FANX III

Department of the Army
Office of Chief of RD&A
Attn: DAMA-WS
DAMA-WSM-A (LTC B. Pellegrini)

Department of the Army
Office of Deputy Chief of Staff
for Operations & Plans
Attn: DAMO-ROD (LTC Mayhew)
DAMO-ROD (LTC Fox)

Ballistic Missile Defense Program
Office (BMDPO)
Attn: Mr. Albert J. Bast, Jr.

Commander, US Army Missile Command
Attn: AMCPM-HEL (Mr. Jennings)
AMCPM-HEL-T (Dr. Evers)

Commander, US Army Missile Command
Attn: AMSMI-RNS

Commanding Officer
US Army Mobility Equipment R&D Center
Attn: AMEFB-MW

Commander, Rock Island Arsenal
Attn: SARRI-LR
Mr. J. W. McGarvey

Commander, US Army Armament Command
Attn: AMSAR-RDT

Director
Ballistic Missile Defense Advance
Technology Center
Attn: ATC-O, Mr. W. O. Davies

Commander, USA Test & Evaluation
Command
Attn: AMSTE-ME (Dr. N. Pentz)

Commander, US Army Materiel Command
Attn: AMCRD-T (Mr. Paul Chernoff)
(Dr. David Stefanye)
(Dr. B. Zarwyn)

Director, US Army Ballistic Research Lab.
Attn: Dr. Robert Eichelberger
Mr. Frank Allen
Dr. E. C. Alcarez

Commandant, US Army Air Defense School
Attn: Air Defense Agency

Commandant, US Army Air Defense School
Attn: ATSA-CD-MS

Commander, US Army Training and
Doctrine Command
Attn: ATCD-CF

Commander, USA Frankford Arsenal
Attn: Mr. M. Elnick (SARFA-FCD)

Commander, US Army Electronics Comman
Attn: AMSEL-CT-L (Dr. R. G. Buser)

Commander
US Army Combined Arms Combat
Developments Activity

Deputy Commandant for Combat &
Training Developments
US Army Ordnance Center and School
Attn: ATSL-CTD-MS-R (LTC Stewart)

Department of the Navy
Office of the Chief of Naval Operations
Attn: CDR L. E. Pellock, USN
(OP-982F3)
Mr. L. E. Triggs (OP-35E)

Office of Naval Research, Boston
Attn: Dr. Fred Quelle

Office of Naval Research, Virginia
Attn: Dr. W. J. Condell (421)

Department of the Navy
Deputy Chief of Naval Materiel (Dev)
Attn: Mr. R. Gaylord (MAT 032B)

Naval Missile Center
Attn: Gary Gibbs (Code 5352)

Commander, Naval Sea Systems Command
Department of the Navy
Attn: Capt. J. G. Wilson, PMS-405

Superintendent, Naval Postgraduate School
Attn: Library (Code 2124)

US Naval Weapons Center, China Lake
Attn: Mr. E. B. Niccum (Code 5114)

Naval Research Lab., Washington, D. C.
Attn: Dr. J. M. MacCallum (Code 5503)
EOTPO
Dr. P. Livingston (Code 5560)
Mr. D. J. McLaughlin (Code 5560)
Dr. J. L. Walsh (Code 5503)
Dr. J. T. Schriempf (Code 6410)
Dr. R. F. Wenzel (Code 6410)
Mr. R. W. Rice (Code 6360)
Dr. L. R. Hettche (Code 6310)
Dr. J. K. Hancock (Code 6110)

Naval Surface Weapons Center, White Oak Lab.
Attn: Dr. E. L. Harris (Code 313)
Dr. L. H. Schindel (Code 310)
Mr. D. L. Merritt (Code 034)
Mr. J. Wack (Code 048)

Hq. AFSC/XRLW, Andrews AFB
Attn: Major James M. Walton

Hq. USAF(RDPS), Washington, D. C.
Attn: LTC A. J. Chiota

Hq. AFSC(DLCAW), Andrews AFB
Attn: Maj. H. Axelrod

Air Force Weapons Lab., Kirtland AFB
Attn: Col. Donald L. Lamberson (AR)
Col. John C. Scholtz (PG)
Col. Russell K. Parson (LR)
Lt. Col. John C. Rich (AL)

Hq. SAMSO, Los Angeles
Attn: Capt. Dorian A. DeMaio (XRTD)
IND
Capt. Thomas J. Ernst (DYD)

AF Avionics Lab. (TEO), Wright
Patterson AFB
Attn: Mr. K. Hutchinson

AF Materials Lab., Wright Patterson AFB
Attn: Maj. Paul Elder (LPJ)
Dr. William Frederick (LPO)

Department of the Air Force
Hq. Foreign Technology Div.
Attn: Mr. R. W. Buxton (ETEO)

AF Aero Propulsion Laboratory
Attn: Maj. George Uhlig (AFAPL/NA)

RADC (OCSE/Mr. R. Urtz), Griffiss AFB

Hq. Electronics Systems Div. (ESD)
Attn: Capt. Allen R. Tobin (XRE)

AF Rocket Propulsion Lab., Edwards AFB
Attn: B. R. Bornhorst (LKCG)

CINCSAC/INEP, Offutt AFB

USAF/INAKA, Washington, D. C.
Attn: LTC Frederic C. Dunlap

Defense Intelligence Agency, Washington,
Washington, D. C.
Attn: Mr. Seymour Berler (DTIA)

Central Intelligence Agency,
Washington, D. C.
Attn: Mr. Julian C. Nall (OSI/PSTD)
Dr. John E. Ashman (OWI/DSD)

Aerodyne Res. Inc., Burlington, MA
Attn: Charles E. Kolb

Analytic Services, Inc., Virginia
Attn: Dr. John Davis

Aerospace Corp., Los Angeles
Attn: Dr. G. P. Millburn
Dr. Walter R. Warren, Jr.
Dr. Elliott L. Katz

Airesearch Manuf. Co., Los Angeles
Attn: Mr. A. Colin Stancliffe

Atlantic Res. Corp., Virginia
Attn: Mr. Robert Naismith

AVCO - Everett Res. Lab., MA
Attn: Dr. George Sutton
Dr. Jack Dougherty

Battelle Columbus Laboratories
Attn: Mr. Fred Tietzel (STOIAC)

Bell Aerospace Co., Buffalo, NY
Attn: Dr. Wayne C. Solomon

Boeing Co.
Attn: Mr. M. I. Gamble
ORGN 2-5006, MS 8C-88

ELS Inc., Sunnyvale, CA
Attn: Mr. Harold A. Malliot

Electro-Optical Systems, Pasadena, CA
Attn: Dr. Andrew Jensen

General Electric Co., Pittsfield, MA
Attn: Mr. D. G. Harrington
Room 1044

General Research Corp., Santa Barbara, CA
Attn: Dr. R. Holbrook

General Research Corp., VA
Attn: Dr. Giles, F. Crimi

Hercules, Inc., Wilmington, DE
Attn: Dr. R. S. Voris

Hercules, Inc., Cumberland, MD
Attn: Dr. Ralph F. Preckel

Hughes Research Labs., Malibu, CA
Attn: Dr. D. Forster
Dr. Arthur N. Chester
Dr. Viktor N. Chester
Dr. Gerald S. Picus

Hughes Aircraft Co., Culver City, CA
Attn: Dr. Eugene Peressini (Bldg. 6, MS/E-125)
Dr. John Fitts (MS 5B-138)
Dr. J. A. Alcalay (Bldg. 6, MS/E-182)

Hughes Aircraft Co., Fullerton, CA
Attn: Dr. William Yates

Institute for Defense Analyses, VA
Attn: Dr. Alvin Schnitzler

Johns Hopkins University
Attn: Dr. Albert M. Stone
Dr. R. E. Gorozdos

Lawrence Livermore Lab., Livermore, CA
Attn: Dr. R. E. Kidder
Dr. E. Teller
Dr. Joe Fleck
Dr. John Emmett
Mr. Carl Haussmann

Los Alamos Scientific Labs.
Attn: Dr. Keith Boyer (MS 530)
Dr. O. P. Judd

Lulejian & Associates, Inc., Torrance, CA

Lockheed Palo Alto Res. Lab.
Attn: L. R. Lunsford
Orgn. 52-24, Bldg. 201

Mathematical Sciences Northwest, Inc., Bellevue, WA
Attn: Mr. Peter H. Rose &
Mr. Abraham Hertzberg

Martin Marietta Aerospace, Denver, CO
Attn: Mr. Roy J. Heyman (Mail No. 048
Dr. Scott Gilles (Mail No. 8105)

Massachusetts Inst. of Technology
Lincoln Lab.
Attn: Dr. S. Edelberg
Dr. L. C. Marquet
Dr. J. Freedman
Dr. G. P. Dinneen
Dr. R. H. Rediker

McDonnell Douglas Astronautics Co.
Huntington Beach, CA
Attn: Mr. P. L. Klevatt
Dept. A3-360-B3GO, M/S 14-1

McDonnell Douglas Res. Labs.
St. Louis, MO
Attn: Dr. D. P. Ames

MITRE Corp., Bedford, MA
Attn: Mr. A. C. Cron

Dr. Anthony N. Pirri
Physical Sciences Inc., Wakefield, MA

Northrop Corp., Hawthorne, CA
Attn: Dr. Gerald Hasserjian
Dr. M. M. Mann

Pacific Sierra Res. Corp.
Attn: Dr. R. Lutomirski

Philco Ford, Newport Beach, CA
Attn: W. H. Rohrer
Air Strike Programs

RAND Corp., Santa Monica, CA
Attn: Dr. Claude R. Culp

Raytheon Co., Waltham, MA
Attn: Dr. Frank A. Horrigan (Res. Div.)

Raytheon Co.
Bedford Labs., Missile Systems Div.
Attn: Dr. H. A. Mehlhorn
Optical Systems Dept.
M/S S4-55

Raytheon Co., Waltham, MA
Attn: Dr. Hermann Statz

Radio Corporation of America
Missile and Surface Radar Div.
Attn: Mr. J. A. Colligan
Information Control

Riverside Research Institute, NY
Attn: Dr. L. H. O'Neill
Dr. John Bose
HPEGL Library

R&D Associates, Inc., Santa Monica, CA
Attn: Dr. R. E. LeLevier
Dr. R. Hundley

Rockwell International Corp., Anaheim, CA
Attn: R. E. Hovda (DB29)
Dr. J. Winocur (D/528, HA14)

Rockwell International Corp.
Rocketdyne Div.
Albuquerque, NM
Attn: Mr. C. K. Kraus, Manager

SANDIA Labs. Albuquerque, NM
Attn: Dr. A. Narath, ORG 5000

W. J. Schafer Associates, Inc.
Wakefield, MA
Attn: Francis W. French

Stanford Research Institute
Menlo Park, CA
Attn: Dr. R. A. Armistead
Mr. J. E. Malick

Science Applications, Inc., La Jolla, CA
Attn: Dr. John Asmus

Science Applications, Inc., Arlington, VA
Attn: Mr. Lawrence Peckham

Science Applications, Inc., Ann Arbor, MI
Attn: Dr. R. E. Meredith

Science Applications, Inc., Bedford, MA
Attn: Dr. Robert Greenberg

Systems Consultants, Inc., Washington, D.C.
Attn: Dr. Robert B. Keller

Systems, Science & Software, La Jolla, CA
Attn: Mr. Alan F. Klein

Thiokol Chemical Co., Wasatch Div.
Attn: Mr. James E. Hansen

TRW Systems Group, Redondo Beach, CA
Attn: Mr. Norman F. Campbell
Mr. Eugene M. Noneman

United Aircraft Res. Lab., East Hartford,
Attn: Mr. G. H. McLafferty
Mr. Albert Angelbeck

United Aircraft Corp., Pratt and Whitney
Acft. Div., Florida R&D Center
Attn: Dr. R. A. Schmidtke
Mr. Ed Pinsley

VARIAN Associates, EIMAC Div.
San Carlos, CA
Attn: Mr. Jack Quinn

Vought Systems Div., LTV Aerospace Corp
Dallax, TX
Attn: Mr. F. G. Simpson
Mail Station 2-54142

Westinghouse Electric Corp.,
Defense and Space Center,
Baltimore, MD
Attn: Mr. W. F. List

Westinghouse Res. Lab.
Pittsburgh, PA
Attn: Dr. E. P. Riedel
Mr. R. L. Hundstad